Journal Name

ARTICLE

Three Coordination Frameworks with Copper Formate based Low Dimensional Motifs: Synthesis, Structure and Magnetic Properties

Sally M. Bovill,[a] Richard J. C. Dixey[b] and Paul J. Saines[a,b*]

Received 00th January 20xx,
Accepted 00th January 20xx

DOI: 10.1039/x0xx00000x

www.rsc.org/

In this study we report the synthesis, crystal structures and magnetic properties of three frameworks wherein Cu cations are bridged by formate linkers into one-dimensional motifs. One of these compounds, $Cu_2(HCO_2)_3(C_3N_2H_4)_4(NO_3)$, contains a ladder motif but remains paramagnetic to 2 K. This is likely because of the longer superexchange pathway along its chains due to the orientation of the Jahn-Teller axis of its Cu cations. In contrast $Cu(HCO_2)(NO_3)(NH_3)_2$ and $Cu(HCO_2)(ClO_4)(NH_3)_2$ feature $Cu(HCO_2)$ chains in which the Jahn-Teller axis is oriented perpendicular to the chain direction; these exhibit antiferromagnetic order below 12 and 7 K, respectively. Their magnetic susceptibilities are well fitted by a one-dimensional chain model but further examination of their magnetic properties reveals significant inter-chain magnetic coupling and a lack of spin dynamics. This suggests that these transitions correspond to the emergence of long-range magnetic order, highlighting the importance of detailed studies of frameworks containing low dimensional motifs to gain a deeper understanding of their magnetic behaviour.

1. Introduction

Coordination frameworks, including dense Metal-Organic Frameworks (MOFs), have attracted significant attention in recent years for their ability to exhibit a wide range of magnetic and electronic functionalities.[1] These are uniquely modified from metal oxides, with which such properties are traditionally associated, because frameworks adopt unique structures due to the structure directing effect of their non-spherical ligands. This often leads to highly anisotropic and low dimensional structures with well-isolated chains and sheets;[2] making them unique windows into exotic states such as spin chains and ladders, which are better isolated than is possible in low dimensional oxides. On the other hand three-dimensional frameworks have been shown to offer unique routes to multiferroic and relaxor ferroelectric materials; their great compositional flexibility gives them tremendous scope for optimisation in this regard.[3,4] Frameworks containing the Cu^{2+} spin ½ cation are of particular interest. From a low dimensional point of view they represent experimental realisations of the most well theoretically studied and most quantum of systems.[5] On the other hand in three-dimensional frameworks the orbital ordering of the Jahn-Teller axis can offer an additional method for symmetry lowering that can offer additional scope for the emergence of functional properties.[6,7]

Building frameworks from small ligands is key to bringing cations close enough together to enable magnetic communication between them, from which order emerges. The formate ligand is arguably the simplest organic ligand available to coordination frameworks. Despite this frameworks containing magnetic cations bridged by this simple ligand have exhibited a wide range of properties from magnetic chains in low dimensional structures to multiferroic behaviour in structures remarkably similar to the perovskite oxides.[3,8-10] The balance between systems that exhibit low dimensional short-range and three-dimensional long-range order appears particularly finely balanced, which can be tipped by factors such as orbital order.[7,11,12] As found for other frameworks, systems that initially appear likely to be low dimensional can instead exhibit long-range magnetic order due to weak through-space interactions between their low dimensional building blocks.[12,13] Alternatively formate-bridged chains and sheets can interact so weakly that these low dimensional units remain paramagnetic even at very low temperatures.

In this work we present the synthesis of three new frameworks, which contain Cu^{2+} cations connected into chains or ladders via the formate ligand, alongside their structural and magnetic characterisation. These low dimensional motifs appear well isolated from each other, and therefore initially appear strong candidates for low dimensional systems. We find, however, that in fact they either exhibit significant interactions beyond their one-dimensional motifs or lack any indication of any magnetic order down to ultra-low temperature, depending partly on the orientation of their Jahn-Teller axis. This highlights the need for continued careful characterisation of apparently

[a] Inorganic Chemistry Laboratory, Department of Chemistry, University of Oxford, Inorganic Chemistry Laboratory, South Parks Road, Oxford, OX1 3QR, UK.
[b] School of Physical Sciences, Ingram Building, University of Kent, Canterbury, CT2 7NH Email: P.Saines@kent.ac.uk

Electronic Supplementary Information (ESI) available: CIFs from single crystal X-ray structure determination (also deposited in the CSD at entries 1492387-1492389) and figures displaying further crystallographic details, powder diffraction patterns, magnetic property measurements, infrared spectra and thermogravimetric analysis are available. See DOI: 10.1039/x0xx00000x

low dimensional frameworks to reveal the true nature of their magnetism.

2. Experimental Section

All three samples were made by slow diffusion reactions, layering solutions of the copper salts above the organic building blocks. $Cu_2(HCO_2)_3(C_3N_2H_4)_4(NO_3)$, hereafter known as **CuFmIm**, was made as part of an extensive but unsuccessful attempt to make a wider family of (Imidazolate)$M(HCO_2)_3$ frameworks.[14] A 5 mL ethanol solution with 0.25 M concentration of H_2CO_2 and 0.25 M imidazole was placed at the bottom of a glass tube with 8 mL of a 0.05 M ethanol solution of $Cu(NO_3)_2{\cdot}2.5H_2O$ layered on top, separated by 2 mL of ethanol. Dark blue needle-like crystals formed after 2 days and were recovered by filtration (49 mg, 41 % yield). $Cu(HCO_2)(NO_3)(NH_3)_2$ (53 mg, 32 % yield), hereafter known as **CuFmNO$_3$**, was made by layering 10 mL of a 0.1 M methanol solution of $Cu(NO_3)_2{\cdot}2.5H_2O$ over 10 mL of a 0.2 M H_2CO_2 and 0.4 M NH_4HCO_2 methanol solution. Dry methanol (<50 ppm H_2O), produced dark blue crystals after a week. Methanol dried over 3A molecular sieves produced light blue crystals, of $Cu(HCO_2)_2$[10] after a week, these were removed by filtration, and dark blue **CuFmNO$_3$** crystals formed after a further 3 weeks (73 mg, 44 %). $Cu(HCO_2)(ClO_4)(NH_3)_2$ (81 mg, 67 %), hereafter known at **CuFmClO$_4$**, was made by layering 10 mL of a 0.05 M $Cu(ClO_4)_2{\cdot}6H_2O$ methanol solution over 10 mL of a 0.1 M H_2CO_2 and 0.2 M NH_4HCO_2 10 mL methanol solution when using dry methanol. This yielded large dark blue rod-shaped crystals after a week. **CuFmClO$_4$** could also be formed by using methanol dried over 3A molecular sieves after a month using the same volumes of these solutions but with concentration of each reagent doubled (61 mg, 25 %).

Structure determination was carried out using a Nonius Kappa CCD using Mo Kα radiation, λ= 0.7107 Å, generated from a conventional source, operating at 60 kV and 30 mA, with a graphite monochromator. Samples were cooled to 150 K using an Oxford Cryosystem cryostream and held in a MiTeGen micro-loop. Full hemispheres of data were collected for each sample and subsequently indexed, integrated and reduced using DENZO/SCALEPACK,[15] with empirical absorption corrections performed using the same packages (see Table 1 for crystallographic details). Structures were solved using direct methods in SHELXS-2008[16] or charge flipping in olex2.solve[17] and refinements subsequently carried out using a least-squares method with SHELXL-2008[16] using the Olex2 graphical user interface[17]. The atomic displacement parameters for non-hydrogen atoms were typically refined anisotropically. The positions of hydrogen atoms were typically geometrically fixed using the AFIX commands in SHELXL-2008[16] and their displacement parameters fixed to being 1.2 times the value of the atom to which they were attached.

Sample phase purity was examined using powder X-ray diffraction carried out on a PANalytical Empyrean diffractometer equipped with monochromated Cu Kα_1, λ = 1.5406 Å, X-rays and using a PIXcel 1D detector. Samples were held on a glass plate at room temperature and the data obtained were subsequently fitted using the Le Bail method in the program Rietica[18] (see Fig. S1-S3). Microanalysis confirmed the purity of these samples and, for **CuFmNO$_3$** and **CuFmClO$_4$**, enabled the clear identification of the presence of ammonia groups. **CuFmIm** was found to be 29.79 % C, 3.27 % H and 20.62 % N *c.f.* to 30.21 % C, 3.21 % H and 21.14 % N expected. **CuFmNO$_3$** was 5.96 % C, 3.31 % H and 20.37 % N *c.f.* to 5.87 % C, 3.45 % H and 20.54 % N. **CuFmClO$_4$** was 5.13 % C, 3.01 % H and 11.45 % N *c.f.* to 4.96 % C, 2.92 % H and 11.57 % N

Magnetic properties of the three samples examined in this study were characterized by Quantum Design magnetometers, either a MPMS 5 or MPMS XL instrument, using 5 T superconducting magnets. Samples were placed in gelatin capsules enclosed inside a pierced straw with a uniform diamagnetic background. Thermal stabilities of **CuFmIm** and **CuFmNO$_3$** were studied using a Perkin-Elmer TGA 7 Thermogravimetric Analyser, with samples held in a platinum plan and heated at 10 °C min^{-1}. Infrared spectra of these two compounds were also measured between 4000 cm^{-1} and 500 cm^{-1} using a Bruker Tensor-27 ATR spectrometer. Infrared spectra and thermogravimetric analysis were, unfortunately, unable to be carried out for **CuFmClO$_4$** due to concerns that compression or heating of this organic perchlorate may trigger the potentially explosive perchlorate anions.

Table 1: Crystallographic data for the structures determined in this work by single crystal X-ray diffraction.

Compound	**CuFmIm**	**CuFmNO$_3$**	**CuFmClO$_4$**
Formula	$Cu_2C_{15}H_{19}N_9O_9$	$CuCH_7N_3O_5$	$CuCH_7N_2O_6Cl$
Formula Weight	596.46	204.64	242.08
T (K)	150(2)	150(2)	150(2)
Crystal System	Orthorhombic	Orthorhombic	Orthorhombic
Space Group	*Pnma*	*Pmnb*	*Pnma*
a (Å)	9.3812(2)	7.1767(3)	7.4087(6)
b (Å)	12.9376(3)	7.3661(4)	7.8568(7)
c (Å)	18.1801(4)	12.3418(7)	12.3745(10)
V (Å^3)	2206.52(8)	652.44(6)	720.30(10)
Z	4	4	4
ρ_{cal} (g cm^{-3})	1.796	2.083	2.232
μ (cm^{-1})	1.99	3.32	3.39
Refl. meas./unique	36934/2637	9265/814	4581/879
Parameters refined	174	59	62
R_1, wR_2[a] (all)	0.1005, 0.2334	0.0734, 0.1872	0.0969, 0.2140
R_1, wR_2[a] (obs)	0.0718, 0.2031	0.0496, 0.1366	0.0534, 0.1266
Goodness of Fit	1.160	1.205	1.177

[a] $w = 1/[\sigma^2(F_o^2) + (aP)^2 + bP]$ and $P = (\max(F_o^2, 0) + 2F_c^2)/3$; $R_1 = \sum||F_o|-|F_c|| / \sum|F_o|$ and $wR_2 = \sqrt{[(F_o^2 - F_c^2)^2 / \sum w(F_o^2)^2]}$

3. Results and Discussion

3.1 Crystal Structures

The three structures reported in this study all adopt *Pnma* orthorhombic symmetry, although **CuFmNO$_3$** is in the *Pmnb* setting of this space group. The structure of **CuFmIm** contains a ladder-like motif in which the Cu cations are bridged by formate ligands (see Fig. 1). These ladders occupy the *ac* plane, running along the *a*-axis in a structure that overall has I^0O^1 connectivity according to the scheme of Cheetham *et al*.[19] Its asymmetric unit contains two Cu cations, two imidazole molecules, three formate anion and one nitrate anion (see Fig. S4). Both crystallographically distinct Cu cations are coordinated, in square-pyramidal geometry, to an oxygen atom from each of the three distinct formate anions and a nitrogen atom from two imidazole ligands, which are arranged in a *trans*-fashion above and below the chains (see Table S1 for selected bond distances).

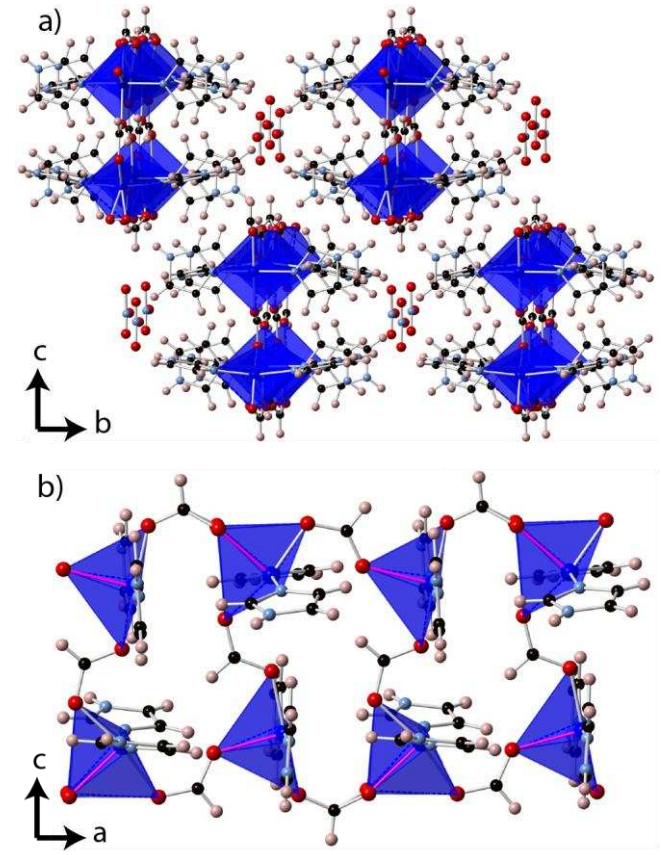

Fig. 1: The structure of **CuFmIm** showing a) the arrangement of ladders in the *bc* plane, interspaced by NO_3^- anions along the *b*-axis and b) a spin ladder in the *ac* plane with the elongated bond along the Jahn-Teller axis highlighted in magneta. The Cu coordination environment is shown in dark blue and the C, N, O and H atoms are black, light blue, red and pink, respectively.

The bond valence sums of the Cu cations in **CuFmIm** are 2.21 and 2.22,[20] consistent with the presence of Cu^{2+}. The distinct Cu cations alternate both across the rung and down the legs of the ladders. The Jahn-Teller axis of the Cu cations lie down the legs, in the case of the Cu1 cation the oxygen atom of the formate ligand to which it has the longest bond is disordered over two positions. The alignment of the Jahn-Teller axis leads to alternating potential superexchange distances of 6.770(18) Å and 6.780(19) Å through the formate linkers down the legs, as opposed to 6.531(16) Å across the rungs. The formate coordination along the chains alternates between *syn-syn* and *syn-anti*, while those in the rungs are *syn-anti*. The crystallographically distinct imidazole ligands alternate down the *a*-axis, with successive imidazoles being rotated close to 90° to each other so they are close to a T-stacked arrangement, suggesting significant π-interactions. The space occupied by the imidazole ligands ensures the copper cations in separate ladders are well separated, with nearest inter-chain Cu-Cu separations of 7.646(1) Å along the ⟨101⟩ directions. The uncoordinated nitrate anions separate the ladders even further along the *c*-axis, leading to nearest Cu-Cu distances of 13.154(1) Å. There is some evidence for disorder of the nitrate anion in **CuFmIm** when the Fourier difference map is examined, which is likely the cause of the larger than normal displacement parameters of the atoms in this moiety. Unfortunately attempts to model this detail were unsuccessful.

CuFmNO$_3$ and **CuFmClO$_4$** adopt very similar structures featuring 1D zig-zag chains of Cu bridged by the formate ligand (see Fig. 2 and Fig. S5) into a I^0O^1 structure.[19] While the asymmetric unit of both structures contain a Cu cation, a formate anion and an ammonia molecule, that of **CuFmNO$_3$** contains an entire nitrate anion while **CuFmClO$_4$** only contains the chloride and three of the four oxygen atoms of the perchlorate anion, with the fourth oxygen required to complete the perchlorate being generated by the *b*-glide (see Fig. S6 and S7).

The Cu cations in both compounds are square-pyramidal coordinated to both distinct oxygen atoms of the formate anion, two ammonia molecules arranged in a *trans*-fashion to each other above and below the chain and the nitrate anion. The longest bond is oriented towards the nitrate anion such that the Jahn-Teller axis of this cation is oriented in the same plane as the chains but not along the chains. The bond valence sum of the Cu cation in **CuFmNO$_3$** is 2.21 while that of **CuFmClO$_4$** is 2.11, consistent with Cu^{2+} (see Table S1 for selected bond distances).[20] This small difference in bond valency is largely due to the longer distance between the Cu and the ClO_4^- anion in **CuFmClO$_4$**, 2.493(8) Å *c.f.* to a Cu-ONO_2 distance of 2.311(7) Å in **CuFmNO$_3$**, suggesting the interaction between the Cu cation and ClO_4^- anion is weaker than with the NO_3^- anion. The likely super-exchange pathway along the chains, through the *syn-anti* formate ligand, is 6.602(16) Å and 6.58(2) Å in **CuFmNO$_3$** and **CuFmClO$_4$,** significantly shorter than that along the legs in **CuFmIm**. The nearest through space Cu-Cu inter-chain distances are between chains in different *bc* planes, which are staggered by half a unit cell along the *c*-axis compared to each other at 5.456(1) Å in **CuFmNO$_3$** and 5.853(2) Å in **CuFmClO$_4$**. The inter-chain separation of the nearest neighbour Cu atoms in the plane of the zig-zag chains is larger, 9.959(1) Å and 10.420(2) Å, in **CuFmNO$_3$** and **CuFmClO$_4$**, respectively; this is because of the NO_3^- and ClO_4^- anions acting as spacers. The most significant intra-chain interactions in **CuFmNO$_3$,** appears to be hydrogen bonds between the three hydrogen atoms of the amine molecule and oxygen atoms of the nitrate or formate anions between neighbouring chains, with N_D-O_A distances of between 3.079(6) Å and 3.162(7) Å and hydrogen bond angles close to 160°. The hydrogen bonding in **CuFmClO$_4$** appears to be much

weaker with two hydrogen atoms from the ammonia group interacting with an oxygen atom of a perchlorate or formate anion with O_D-O_A distances of 3.171(9) Å and 3.219(8) Å and bond angles close to 150°. A third ammonia hydrogen atom in **CuFmClO$_4$** has a bifurcated bond with oxygen atoms from perchlorates in distinct chains with distances of 3.168(9) Å and 3.225(9) Å and bond angles of less than 130°.

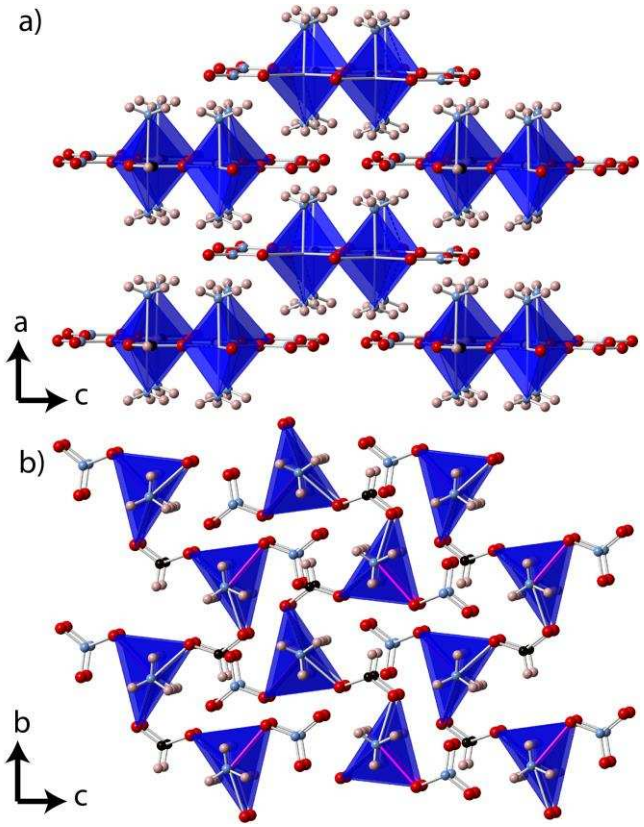

Fig. 2: The structure of **CuFmNO$_3$** showing a) the arrangement of zig-zag chains down the *b*-axis and b) interdigitated chains in the *bc* plane. The colours are the same as in Fig. 1.

3.2 Magnetic Properties

Direct current (DC) magnetic susceptibility measurements were carried out on all compounds created during this study. Zero-field cooled (ZFC) and field cooled (FC) measurements of **CuFmIm** in a 0.1 kOe field suggest the material remains paramagnetic to 2 K (see Fig. 3). This is consistent with isothermal magnetization measurements conducted at 2 K, which approach saturation above 25 kOe (see Fig. 3 insert). Magnetic susceptibility cannot be well fitted using the Curie-Weiss law, requiring the addition of a temperature independent component of the form $\chi = C/(T - T_C) + A$. An excellent fit was obtained with such a model to the 100 Oe ZFC with T_c = 1.13(3) K, C = 0.529(3) emu K mol^{-1} Oe^{-1} and A = 1.20(7) × 10^{-3} emu mol^{-1} Oe^{-1} (see Fig. S8). This suggests that the magnetic interactions in this material are, if any, weak and ferromagnetic. The effective magnetic moment is then 2.06 μ_B, higher than the 1.73 μ_B expected for spin-only Cu^{2+} but in agreement with typical values reported for Cu^{2+} cations.

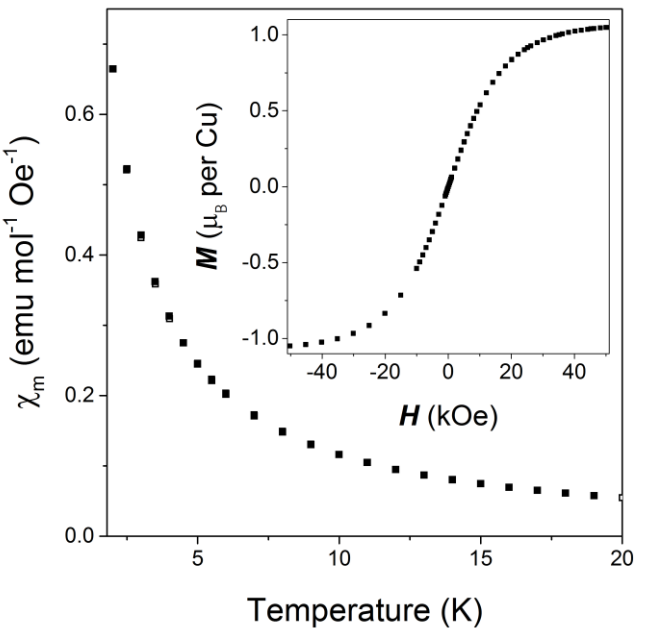

Fig. 3: Magnetic susceptibility of **CuFmIm** measured in a 0.1 kOe field with FC and ZFC susceptibilities are marked with filled and hollow symbols, which largely overlap is this figure. The insert shows isothermal magnetization measurements recorded at 2 K.

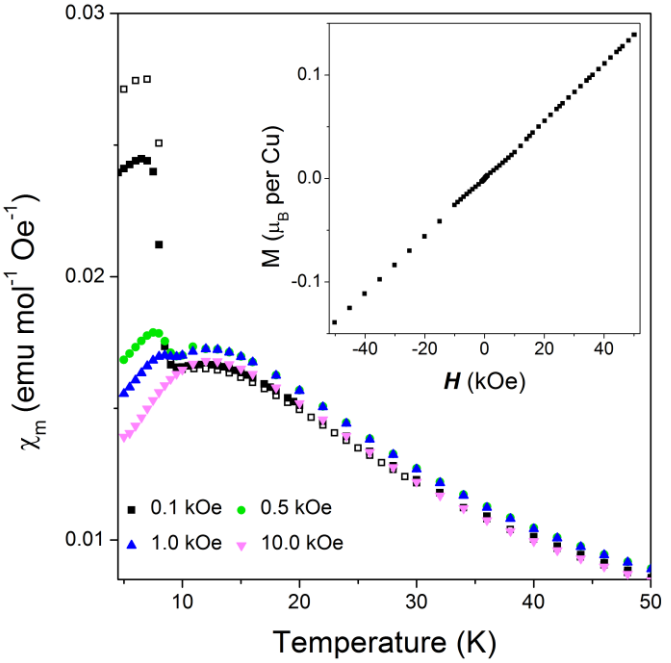

Fig. 4: Magnetic susceptibility of **CuFmNO$_3$** with FC and ZFC susceptibilities marked with filled and hollow symbols. The insert shows isothermal magnetization measurements recorded at 2 K.

In contrast ZFC and FC magnetic susceptibility measurements of **CuFmNO$_3$** carried out at 0.1 kOe exhibit a maximum at 12 K, suggesting the onset of antiferromagnetic order (see Fig. 4). Susceptibility then increases again around 9 K, although the magnitude of this response decreases significantly with applied magnetic field in FC measurements and is completely suppressed in measurements conducted about 10 kOe.

Isothermal magnetization measurements conducted at 2 K do not show any signs of hysteresis and are far from saturation at 50 kOe (see Fig. 4 insert). On this basis we suggest that the behaviour observed below 9 K is likely a result of a trace amount of a magnetic impurity, not observable by powder X-ray diffraction. Alternatively it is also entirely possible it is caused by the emergence of spin canting below 9 K leading to a weak ferromagnetic state, possibly due to spin canting. As for **CuFmIm** it was not possible to fit the 100 Oe magnetic susceptibility data above the antiferromagnetic ordering temperature with a Curie-Weiss model but, instead, a model with a temperature independent component was required. This gave excellent fits with values of A = 6.1(2) × 10^{-4} emu mol^{-1} Oe^{-1}, C = 0.500(4) emu K mol^{-1} Oe^{-1} and T_c = -13.9(0.3) K, consistent with an antiferromagnetic material (see Fig. S9). This gives an effective magnetic moment of 2.00 μ_B, similar to **CuFmIm**, which has the same coordination geometry.

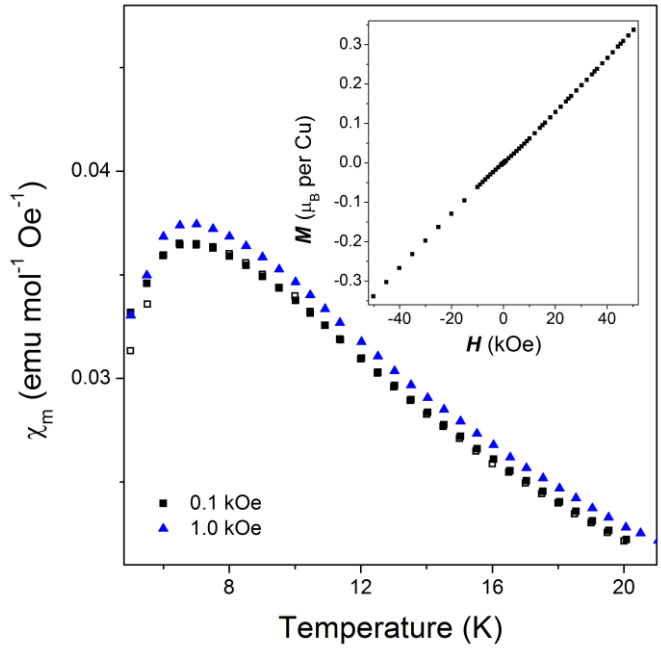

Fig. 5: Magnetic susceptibility of **$CuFmClO_4$** with FC and ZFC susceptibilities marked with filled and hollow symbols, which overlap above 7 K. The insert shows isothermal magnetization measurements recorded at 5K.

Magnetic susceptibility measurements of **$CuFmClO_4$** show a maximum at about 7 K. This is consistent with the emergence of a similar antiferromagnetic state to that found in **$CuFmNO_3$** (see Fig. 5), although its lower onset temperature indicates that the coupling in $CuFMClO_4$ is weaker. This is further supported by isothermal magnetization measurements at 5 K that show no hysteresis and are far from saturation at 50 kOe. The modified Curie-Weiss model used for the other two compounds in this study were also used here giving A = -5.2 (7) × 10^{-4} emu mol^{-1} Oe^{-1}, C = 0.608(8) emu K mol^{-1} Oe^{-1} and T_c = -7.4(2) K (see Fig. S10). This is consistent with antiferromagnetic order at the temperature observed suggesting as for **$CuFmNO_3$**, **$CuFmClO_4$** is well modelled by mean field theory. The effective magnetic moment derived from this fit is 2.21 μ_B.

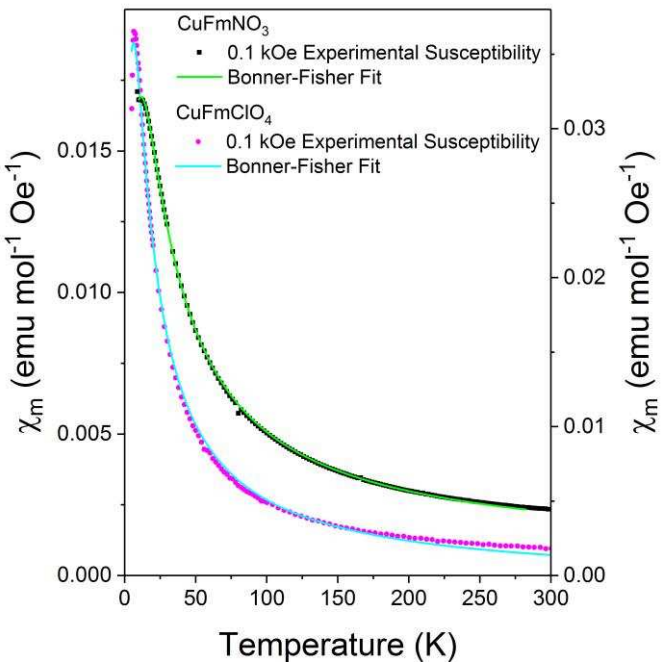

Fig. 6: Bonner-Fisher fits to magnetic susceptibility measurements at 0.1 kOe measured for **$CuFmNO_3$** and **$CuFmClO_4$**. The R^2 of the fits are 0.9999 and 0.9978.

Given both **$CuFmNO_3$** and **$CuFmClO_4$** have chain like structures and magnetically order, we attempted to fit the magnetic susceptibility with the well established Bonner-Fisher[21] approximation for a 1D Heisenberg chain. Allowing for the temperature independent component to the magnetism identified in the Curie-Weiss fits this takes the formulism:

$$\chi = \frac{N_A g^2 \mu_B^2}{k_B T} \times \frac{0.25 + 0.074975x + 0.075236x^2}{1 + 0.9931x + 0.172135x^2 + 0.757825x^3} + A$$

where $x = |J|/k_B T$. Good fits were obtained to the 100 Oe ZFC susceptibility of **$CuFmNO_3$** and **$CuFmClO_4$** using this model (see Fig. 6). This gave values of J/k_B = 17.81(5) K, g = 2.293(3) and A = 6.58(9) × 10^{-4} emu mol^{-1} Oe^{-1} for **$CuFmClO_4$** while J/k_B = 9.76(11) K, g = 2.540(11) and A = -5.9(9) × 10^{-4} emu mol^{-1} Oe^{-1} for **$CuFmClO_4$**. The inter-chain coupling, J', in weakly coupled chains in a quasi one-dimensional spin system can be estimated by the chain mean-field theory of Schulz[22] via:

$$|J'| = \frac{T_N}{4 \times 0.32\sqrt{\ln(5.8J/T_N)}}$$

where T_N is the Néel temperature. On this basis J' is approximately 6.4 K and 3.8 K for **$CuFmNO_3$** and **$CuFmClO_4$**, respectively, which gives similar J'/J ratios of 0.36 and 0.39. This suggests that while **$CuFmNO_3$** and **$CuFmClO_4$** are predominantly one-dimensional, they are far from the isolated 1D limit.

To probe the extent of one-dimensional behaviour in these materials alternating current (AC) measurements on **$CuFmNO_3$** were carried out to examine if there were any dynamics consistent with spin chain behaviour. For measurements carried out in an applied field of 3 Oe, there was no significant frequency dependence observed in the antiferromagnetic cusp in the susceptibility centred at 12 K (see Fig. 7). There is also no

significant phase shift, φ, in this temperature range. This result is consistent with the significant inter-chain interactions suggested by chain mean-field theory, but is nevertheless surprising given the strong one-dimensional structure of the framework.

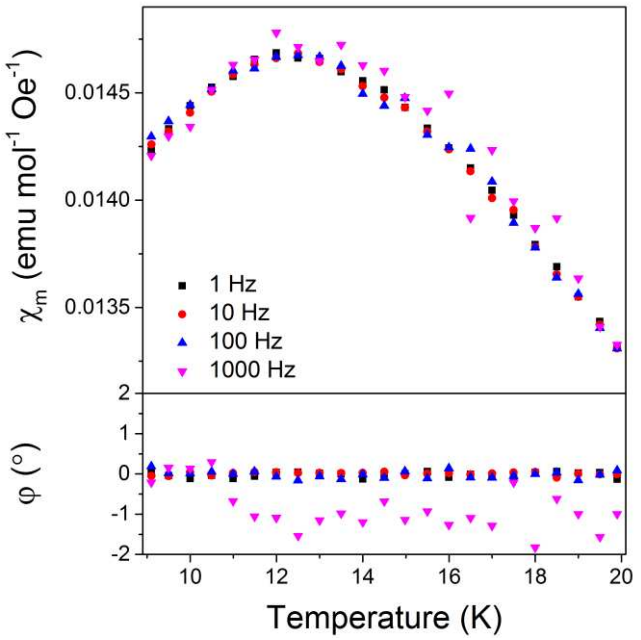

Fig. 7: AC magnetic susceptibility measurements of **CuFmNO$_3$** measure at 3 Oe showing total χ_m (top panel) and $\varphi = \tan^{-1}(\chi_m''/\chi_m')$ (bottom panel).

Interpreting the magnetic susceptibility measurements as indicating that **CuFmNO$_3$** and **CuFmClO$_4$** have long-range order below 12 K and 7 K, we can now explain the differences in their magnetic ordering temperature. While there are no significant differences in bond distances or angles within the one-dimensional chains in these materials the intra-chain distances are about 0.5 Å larger in **CuFmClO$_4$** than **CuFmNO$_3$** due to the larger size of the ClO_4^- anion compared to NO_3^-. This greater distance is consistent with the lower T_N observed. The stronger interaction of the Cu cations with the NO_3 anions in **CuFmNO$_3$** compared to the ClO_4 anions in **CuFmClO$_4$** (*c.f.* Cu-O bond distances of 2.311(7) and 2.493(8) Å, respectively) may also play a subtle role in strengthening the 1D magnetic interactions, as indicated by the Bonner-Fisher[21] fits. The additional electron withdrawing effects from the weakly bonded NO_3 anions should make the Cu cation relatively more electronegative in **CuFmNO$_3$**. This could subtly increase the covalency of the Cu-O bonds within the 1D chains, increasing the strength of superexchange interactions since the pathway remains very similar.

The nature of the magnetic interactions between the chains in **CuFmNO$_3$** and **CuFmClO$_4$** is not obvious. At the magnetic ordering temperature the superexchange interactions within the magnetic chains likely lead to these ordering and this may trigger order of neighbouring chains as a result of many through-space dipole-dipole interactions. If this is the case the number of interactions between chains must compensate for the relative weakness of dipole-dipole interactions. While other formate frameworks are known that are structurally 1D e.g. $NH_4MCl_2(HCO_2)$, where M = Fe, Co and Ni,[9,12] to the best of our knowledge chain mean-field analysis has only been carried out for two formate compounds, $(C(NH_2))_3Cu(HCO_2)_3$[7] and $((CH_3)_2NH_2)Cu(HCO_2)_3$[11]. These both adopt perovskite-like structures and their low dimensional magnetism arises from the orientation of the Jahn-Teller axis of the Cu cations. Despite this these frameworks appear closer to the 1D Heisenberg limit than either **CuFmNO$_3$** or **CuFmClO$_4$**, with J'/J ratios of 0.12 and 0.07 reported for $(C(NH_2))_3Cu(HCO_2)_3$[7] and $((CH_3)_2NH_2)Cu(HCO_2)_3$[11]. This emphasises the importance of analysing the magnetic properties of low dimensional magnets in detail as more superficial examinations of the magnetic properties of such systems coupled with an examination of their structures is not adequate to fully understand their magnetic properties.

The likely reason for **CuFmIm** failing to order at all deserves comment, although it is difficult to be certain of the causes of these differences. The Cu^{2+} coordination environment in all compounds is similar and, as discussed above, the chains in **CuFmNO$_3$** and **CuFmClO$_4$** are connected by formates in *syn-anti* coordination modes as opposed to the *syn-syn* and *syn-anti* found in **CuFmIm**. *Syn-anti* coordination typically mediates the weakest coupling of the three possible coordination modes for a formate ligand bound to two cations so this is unlikely to be the cause of the difference in ordering temperature.[23,24] It therefore seems most likely that magnetic ordering in **CuFmIm** is supressed because, unlike **CuFmNO$_3$** and **CuFmClO$_4$**, the Jahn-Teller axis of its Cu cations are aligned down its chains, increasing the superexchange coupling distance. It is unfortunate that there is no significant magnetic interactions in **CuFmIm** because, to the best of our knowledge, it is the only spin-1/2 formate framework that adopts a ladder-motif; although a diamagnetic Ag(I) formate framework, $Ag(CHO_2)$(4,4'-bipyridine)$\cdot H_2O\cdot H_2CO_2$,[25] and a formate framework containing a more complex ladder motif in which Ni-imidazolate cages make up the nodes of the ladder,[26] have been reported.

3.3 Thermal Stability and Infrared Analysis

Thermogravimetric analysis of **CuFmIm** and **CuFmNO$_3$** indicated these decomposed above 140 and 160 °C, respectively (see Fig. S11 and 12). The decomposition temperatures of these materials were similar regardless of whether the samples were heated under air or N_2. This suggests that the decomposition is primarily thermally driven rather than occurring as a result of the oxidation of the frameworks. In air these materials decompose to ultimately give CuO in a poorly separated multistep process, which makes identification of any intermediates difficult; the process is similar but incomplete in N_2.

Infrared spectra for **CuFmIm** and **CuFmNO$_3$** are presented in Fig. S13 and S14 along with assignment of observed peaks to likely functional groups. Clear evidence for the presence of imidazole is observed in the spectra of **CuFmIm** with =N-H stretches noted at 3320 cm^{-1} and a number of C=C and C=N stretches present between 1542 and 1440 cm^{-1}. Three N-H stretches are observed at 3334, 3271 and 3193 cm^{-1} in **CuFmNO$_3$**. The characteristically strong C=O stretch is observed

in both at 1629 and 1639 cm^{-1}, for **CuFmIm** and **$CuFmNO_3$** respectively. The N=O stretching frequency of **$CuFmNO_3$** is lower than for **CuFmIm** (*c.f.* 1564 cm^{-1} to 1581 cm^{-1}) consistent with the nitrate anion bonding weakly to Cu in **$CuFmNO_3$** but not in **CuFmIm**. Unfortunately C-O stretches from bound formate ligands are expected to appear around 1350 cm^{-1}, which overlaps with the broad region in which N-O stretches and, for **CuFmIm**, =C-H and =N-H bends are expected to appear.[23] Indeed a number of peaks are noted in this region, particularly for **CuFmIm**, and it is therefore difficult to determine with any certainty what features in this region arise from the formate anion, obscuring spectroscopic evidence of the presence of formates with different coordination geometries.

4. Conclusions

In this study we have reported the synthesis, crystal structure and magnetic properties of three Cu formate-based frameworks. We find that one of these compounds, **CuFmIm**, contains a ladder motif in its structure but examination of its magnetic properties shows that it remains paramagnetic to 2 K. In contrast the other two compounds, **$CuFmNO_3$** and **$CuFmClO_4$**, have isostructural one-dimensional chains in their architectures and exhibit antiferromagnetic order below 12 and 7 K, respectively. The Jahn-Teller axis of the Cu cations in **$CuFmNO_3$** and **$CuFmClO_4$** do not lie along the chain direction, unlike **CuFmIm,** which may suppress the magnetic order of the latter compound. While the magnetic susceptibility of **$CuFmNO_3$** and **$CuFmClO_4$** can be well fitted with a Bonner-Fisher 1D chain model, often interpreted as an indication that compounds are low dimensional, we find from chain mean-field theory that the inter-chain interactions are significant, about a third of the strength of intra-chain coupling. The lack of obvious dynamics in the magnetic ordering of **$CuFmNO_3$**, as probed by AC magnetic susceptibility, is consistent with these transitions corresponding to the emergence of long-range magnetic order; this is in keeping with the lower ordering temperature of **$CuFmClO_4$**, given its greater inter-chain spacing. This highlights the importance of a thorough characterization of frameworks with low dimensional motifs to establish their magnetic behaviour.

Acknowledgements

We would like to thank Amber Thompson for help with single crystal X-ray diffraction. The authors would like to thank the Glasstone Trust for funding via the provision of a fellowship.

References

1. a) A. K. Cheetham and C. N. R. Rao, *Science*, 2007, **318**, 58-59; b) C. N. R. Rao, A. K. Cheetham and A. Thirumurugan, *J. Phys.: Condens. Matter*, 2008, **20**, 083202; c) M. Kurmoo, *Chem. Soc. Rev.*, 2009, **38**, 1353-1379; d) M.-H. Zeng, Y.-L. Zhou, W.-X. Zhang, M. Du and H.-L. Sun, *Cryst. Growth Des.*, 2010, **10**, 20-24; e) Z. Yin, Q.-X. Wang and M.-H. Zeng, *J. Am. Chem. Soc.*, 2012, **134**, 4857-4863; f) G. Lorusso, J. W. Sharples, E. Palacios, O. Roubeau, E. K. Brechin, R. Sessoli, A. Rossin, F. Tuna, E. J. L. McInnes, D. Collison and M. Evangelisti, *Adv. Mater.*, 2013, **25**, 4653-4656.
2. a) I. Gil de Muro, F. A. Mautner, M. Insausti, L. Lezama, M. I. Arriortua and T. Rojo, *Inorg. Chem.*, 1998, **37**, 3243-3251; b) P. D. C. Dietzel, Y. Morita, R. Blom and H. Fjellvåg, *Angew. Chem. Int. Ed.*, 2005, **44**, 6354-6358; c) E. Burzurí, J. Campo, L. R. Falvello, E. Forcén-Vázquez, F. Luis, I. Mayoral, F. Palacio, C. Sáenz de Pipaón and M. Tomás, *Chem. Eur. J.,* 2011, **17**, 2818-2822; d) B. Gil-Hernandez, P. Gili, J. Pasan, J. Sanchiz and C. Ruiz-Perez, *CrystEngComm*, 2012, **14**, 4289-4297; e) Y.-Q. Wang, Q. Yue, Y. Qi, K. Wang, Q. Sun and E.-Q. Gao, *Inorg. Chem.*, 2013, **52**, 4259-4268; f) P. J. Saines, J. A. M. Paddison, P. M. M. Thygesen and M. G. Tucker, *Mater. Horiz.*, 2015, **2**, 528-535.
3. a) P. Jain, V. Ramachandran, R. J. Clark, H. D. Zhou, B. H. Toby, N. S. Dalal, H. W. Kroto and A. K. Cheetham, *J. Am. Chem. Soc.*, 2009, **131**, 13625-13627; b) G. Rogez, N. Viart and M. Drillon, *Angew. Chem. Int. Ed.*, 2010, **49**, 1921-1923; c) Z. Wang, K. Hu, S. Gao and H. Kobayashi, *Adv. Mater.*, 2010, **22**, 1526-1533; d) B. Zhou, Y. Imai, A. Kobayashi, Z.-M. Wang and H. Kobayashi, *Angew. Chem. Int. Ed.*, 2011, **50**, 11441-11445; e) L. C. Gómez-Aguirre, B. Pato-Doldán, J. Mira, S. Castro-García, M. A. Señarís-Rodríguez, M. Sánchez-Andújar, J. Singleton and V. S. Zapf, *J. Am. Chem. Soc.*, 2016, **138**, 1122-1125.
4. a) G.-C. Xu, W. Zhang, X.-M. Ma, Y.-H. Chen, L. Zhang, H.-L. Cai, Z.-M. Wang, R.-G. Xiong and S. Gao, *J. Am. Chem. Soc.*, 2011, **133**, 14948-14951; b) L. C. Gómez-Aguirre, B. Pato-Doldán, A. Stroppa, S. Yáñez-Vilar, L. Bayarjargal, B. Winkler, S. Castro-García, J. Mira, M. Sánchez-Andújar and M. A. Señarís-Rodríguez, *Inorg. Chem.*, 2015, **54**, 2109-2116;.
5. a) E. Dagotto and T. M. Rice, *Science*, 1996, **271**, 618-623; b) D. C. Dender, P. R. Hammar, D. H. Reich, C. Broholm and G. Aeppli, *Phys. Rev. Lett.*, 1997, **79**, 1750-1753; c) F. H. L. Essler, A. Furusaki and T. Hikihara, *Phys. Rev. B*, 2003, **68**, 064410; d) P. Abbamonte, G. Blumberg, A. Rusydi, A. Gozar, P. G. Evans, T. Siegrist, L. Venema, H. Eisaki, E. D. Isaacs and G. A. Sawatzky, *Nature*, 2004, **431**, 1078-1081; e) S. L. Drechsler, O. Volkova, A. N. Vasiliev, N. Tristan, J. Richter, M. Schmitt, H. Rosner, J. Málek, R. Klingeler, A. A. Zvyagin and B. Büchner, *Phys. Rev. Lett.*, 2007, **98**, 077202; f) Y. Savina, O. Bludov, V. Pashchenko, S. L. Gnatchenko, P. Lemmens and H. Berger, *Phys. Rev. B*, 2011, **84**, 104447.
6. A. Stroppa, P. Jain, P. Barone, M. Marsman, J. M. Perez-Mato, A. K. Cheetham, H. W. Kroto and S. Picozzi, *Angew. Chem. Int. Ed.*, 2011, **50**, 5847-5850.
7. K.-L. Hu, M. Kurmoo, Z. Wang and S. Gao, *Chem. Eur. J.*, 2009, **15**, 12050-12064.
8. J. L. Manson, J. G. Lecher, J. Gu, U. Geiser, J. A. Schlueter, R. Henning, X. Wang, A. J. Schultz, H.-J. Koo and M.-H. Whangbo, *Dalton Trans.*, 2003, 2905-2911.
9. J. T. Greenfield, S. Kamali, N. Izquierdo, M. Chen and K. Kovnir, *Inorg. Chem.*, 2014, **53**, 3162-3169.
10. F. Sapina, M. Burgos, E. Escriva, J. V. Folgado, D. Marcos, A. Beltran and D. Beltran, *Inorg. Chem.*, 1993, **32**, 4337-4344.
11. Z. Wang, P. Jain, K.-Y. Choi, J. van Tol, A. K. Cheetham, H. W. Kroto, H.-J. Koo, H. Zhou, J. Hwang, E. S. Choi, M.-H. Whangbo and N. S. Dalal, *Phys. Rev. B*, 2013, **87**, 224406.
12. J. T. Greenfield, V. Ovidiu Garlea, S. Kamali, M. Chen and K. Kovnir, *J. Solid State Chem.*, 2016, **236**, 222-229.
13. a) P. J. Saines, J. R. Hester and A. K. Cheetham, *Phys. Rev. B*, 2010, **82**, 144435; b) L. L. L. Sousa, G. F. Barbosa, F. L. A. Machado, L. R. S. Araujo, P. Brandao, M. S. Reis and D. L. Rocco, *IEEE Trans. Magnet.*, 2013, **49**, 5610-5615; c) P. J. Saines, P. T. Barton, M.

Jura, K. S. Knight and A. K. Cheetham, *Mater. Horiz.*, 2014, **1**, 332-337;
14. B.-Q. Wang, H.-B. Yan, Z.-Q. Huang and Z. Zhang, *Acta Crystallogr.*, 2013, **C69**, 616-619.
15. Z. Otwinowski and W. Minor, in *Methods Enzymol.*, ed. Charles W. Carter, Jr., Academic Press, 1997, vol. 276, pp. 307-326.
16. G. Sheldrick, *Acta Crystallog.*, 2008, **A64**, 112-122.
17. O. V. Dolomanov, L. J. Bourhis, R. J. Gildea, J. A. K. Howard and H. Puschmann, *J. Appl. Crystallogr.*, 2009, **42**, 339-341.
18. B. A. Hunter and C. J. Howard, *A computer program for Rietveld analysis of X-ray and neutron powder diffraction patterns,*, Lucas Heights Laboratories, 1998.
19. A. K. Cheetham, C. N. R. Rao and R. K. Feller, *Chem. Commun.*, 2006, 4780-4795.
20. N. E. Brese and M. O'Keeffe, *Acta Crystallogr.*, 1991, **B47**, 192-197.
21. J. C. Bonner and M. E. Fisher, *Phys. Rev.*, 1964, **135**, A640-A658.
22. H. J. Schulz, *Phys. Rev. Lett.*, 1996, **77**, 2790-2793.
23. S. M. Bovill and P. J. Saines, *CrystEngComm*, 2015, **17**, 8319-8326.
24. a) E. Colacio, J. M. Domínguez-Vera, M. Ghazi, R. Kivekäs, M. Klinga and J. M. Moreno, *Eur. J. Inorg. Chem.*, 1999, **1999**, 441-445; b) S. K. Dey, B. Bag, K. M. Abdul Malik, M. S. El Fallah, J. Ribas and S. Mitra, *Inorg. Chem.*, 2003, **42**, 4029-4035; c) Z. Duan, Z. Wang and S. Gao, *Dalton Trans.*, 2011, **40**, 4465-4473;.
25. D.-Q. Zhang, W.-H. Zhang, Q.-F. Xu, J.-P. Lang and S. W. Ng, *Acta Crystallogr.*, 2004, **E60**, m1256-m1258.
26. D. Luo, X.-P. Zhou and D. Li, *Inorg. Chem.*, 2015, **54**, 10822-10828.

